Aluminum Heat Sink Assisted Air-Cooling Thermal Management System for High Current Applications in Electric Vehicles

Hamidreza Behi
ETEC Dept. & MOBI Research Group,
Vrije Universiteit Brussels (VUB),
Brussels, Belgium
Flanders Make, Heverlee, Belgium
Hamidreza.Behi@vub.be

Danial Karimi
ETEC Dept. & MOBI Research Group,
Vrije Universiteit Brussels (VUB),
Brussels, Belgium
Flanders Make, Heverlee, Belgium
Danial.Karimi@vub.be

Joris Jaguemont
ETEC Dept. & MOBI Research Group,
Vrije Universiteit Brussels (VUB),
Brussels, Belgium
Flanders Make, Heverlee, Belgium
Joris.Jaguemont@vub.be

Foad.H.Gandoman
ETEC Dept. & MOBI Research Group,
Vrije Universiteit Brussels (VUB),
Brussels, Belgium
Flanders Make, Heverlee, Belgium
Foad.heidari.Gandoman@vub.be

Sahar Khaleghi
ETEC Dept. & MOBI Research Group,
Vrije Universiteit Brussels (VUB),
Brussels, Belgium
Flanders Make, Heverlee, Belgium
Sahar.Khaleghi@vub.be

Joeri Van Mierlo
ETEC Dept. & MOBI Research Group,
Vrije Universiteit Brussels (VUB),
Brussels, Belgium
Flanders Make, Heverlee, Belgium
Joeri.Van.Mierlo@vub.be

Maitane Berecibar
ETEC Dept. & MOBI Research Group,
Vrije Universiteit Brussels (VUB),
Brussels, Belgium
Flanders Make, Heverlee, Belgium
Maitane.Berecibar@vub.be

***Abstract*—Lithium-ion (Li-ion) batteries are preferred energy storage systems for vehicular applications due to the high capacity, long life, and power density. This paper offers the concept of a hybrid thermal management system (TMS), including a prismatic cell embedded fin heat sink (CHS) for high current applications. The experimental tests and numerical simulations are done to investigate the thermal characteristic of the utilized battery and CHS in natural and forced convection in 8C discharging rate (184 A). Results indicate that the maximum cell temperature in natural convection (NC) reaches 56 °C. Moreover, the temperature of the CHS in natural and forced convection reaches 51.5 °C and 31.1 °C. For further investigation, the optimization, including three cases, is done for the geometry of the forced convection cooling box. Results indicate that the maximum temperature of the CHS compared with NC reduced by 39.6%, 40.9%, and 38.4% for cases A, B, and C, respectively. In addition, there is an improvement of 6%, 28%, and 36% in the cell temperature uniformity for cases A, B, and C, respectively. It is also found that the inlet velocity of 3 m/s preserves the CHS in a safe temperature zone, which decreases the fan power consumption by 50%.**

Keywords— Lithium-ion battery, Thermal management system, Heat sink, Air cooling, Optimization

I. INTRODUCTION

RECENTLY, the energy storage and rechargeable batteries are in the center of attention due to the negative effects of fossil fuels on global warming and the attempts to prevent them. Among all kinds of rechargeable batteries, Li-ion cells have received more attention, owing to high power density, life cycling time, reliability, and durability compared with other kinds of rechargeable batteries [1]. However, they are very sensitive to increase temperature. Several studies have demonstrated that increasing the temperature of the Li-ion battery cells, speeds up capacity degradation, and shortens battery lifetime [2], [3]. Therefore, some studies are carried out to discover new approaches to keep the temperature of Li-ion batteries in a safe zone.

The safe temperature zone for Li-ion batteries is defined between 25-40 [4]–[6]. There are different active and passive methods for thermal management of Li-ion batteries that comprise air cooling, liquid cooling, heat pipe, and phase change material (PCM) [7], [8]. Air cooling is one of the conventional techniques in many cooling applications due to its simplicity. Generally, it is divided into natural and forced air cooling. Chen et al. [9] designed an operative symmetrical air-cooled thermal management system with desirable cooling performance and low energy consumption. Fan et al. [10] experimentally studied the air cooling of the battery pack, which consists of 32 cylindrical batteries.

However, most air-cooling systems are inefficient due to low air heat transfer of coefficient. Generally, the liquid cooling system is the most capable and functional cooling approach, which is used in a variety of cooling applications [11], [12]. Lai et al. [13] constructed an innovative light-weight liquid cooling thermal management system for a cylindrical Li-ion battery pack. Kong et al. [14] designed an original liquid cooling system coupling with PCM for thermal management of cylindrical cells in different ambient temperatures. Nevertheless, the liquid cooling systems are massive and work with the high investment cost, high power consumption, and ample space occupation. Moreover, they

978-8-8872-3749-8 ©2020 AEIT

suffer from the liquid leakage. PCM is a common passive method for cooling and energy storage in different industrial applications [15]. The combination of PCM with Nanomaterial [16]–[18], graphite, and Nanocarbon tube is also used for cooling and energy storage applications. Heyhat et al. [19] studied the cooling effect of PCM and Nano PCM on the performance of the cylindrical Li-ion battery in the high heat generation rate condition. Safdari et al. [20] numerically investigated the effect of PCM and air cooling on the 12 cylindrical cells.

However, all PCMs have low thermal conductivity and the leaking problem. Moreover, they are not practical in high current and stressful conditions. Heat pipe and fin is also another common passive cooling method that widely used in many cooling applications [21], [22]. Behi et al. [23] experimentally considered the effect of heat pipe with the air and liquid cooling method for Li-ion batteries. Behi et al. [24] experimentally and numerically considered the effect of L shaped heat pipe on the cooling performance of a cylindrical battery module.

Nevertheless, all heat pipes suffer a complicated design, high cost, and sensitive structures to gravity. In high current applications, most battery thermal management systems are not able to control the cell temperature in the safe zone. Moreover, they suffer from temperature non-uniformity in the cell/module level. Consequently, a costly and massive cooling system embedded with many heat pipes and cooling plates is necessary to control the temperature of the battery module/pack [25], [26]. Therefore, the need for an efficient, light, inexpensive, and simple cooling system is necessary for high current applications.

In this paper, the effect of folded aluminum fin heat sink assisted air cooling is considered. Natural and forced air cooling is the simplest way based on cost, weight, and space limitation to achieve cooling performance. The cell temperature experimentally is considered in NC. The aluminum heat sink is used to compensate for the low heat transfer coefficient of air. To increase the cooling efficiency, the heat sink is connected to the critical zone (hottest zone) of the cell. To investigate the thermal performance of the cell, the CFD model using COMSOL Multiphysics has been employed in the transient simulation process. The surface temperatures of the lithium-titanite (LTO) cell in natural and forced convection are obtained through experiments to guarantee the accuracy of the simulation model. To reach the efficient design to control the maximum temperature of the cell, increase temperature uniformity and decrease the power consumption of the system, several optimizations are done.

II. EXPERIMENTAL SETUP

A. Battery Overview Description

In the present study, the thermal performance of an LTO cell experimentally and numerically is considered in the 8C discharging rate (184 A). The main features of the prismatic LTO-based cell are reported in Table 1.

TABLE I
THE MAIN PROPERTIES OF THE CELL

Symbol	Quantity	Value
-	Chemistry	LTO
-	Shape	Prismatic
V	Nominal Voltage	2.3
V	Maximum Voltage	2.7
V	Minimum Voltage	1.5
Ah	Capacity	23
-	Specific Energy	23
-	Energy Density	202
kg	Weight	0.55
L	Volume	0.26
mm	Dimensions L×W×H	115×22×103
J/kg.K	Heat Specific Capacity	1150
W/m.K	Thermal Conductivity (x,y,z)	31, 0.8, 31

V=volt, Ah=Ampere hour, kg=kilogram, L=Liter, J=Joules, K=Kelvin, W=Watts, m=meters

B. Test Setup Description

To investigate a light, inexpensive, and effective air-cooling system, an LTO prismatic battery cell embedded with an aluminum heat sink. The selected fin heat sink is a kind of folded heat sink which is considered for high-power and forced convection applications with limited space, to enlarge

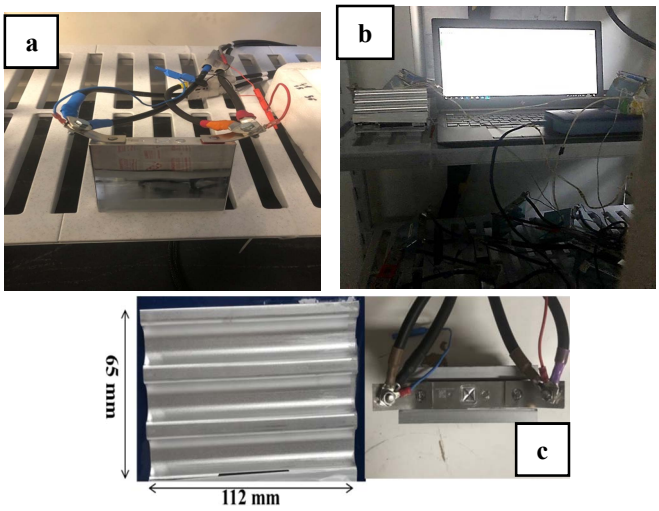

Fig. 1. a) The test set up, b) the picture of LTO cell embedded with cooling heat sink in NC, c) the Aluminum heat sink dimensions

the surface area without increasing the heat sink volume. The main characteristic of the folded fin heat sinks is the usage of light-weight cooling fins that leads to a high cost and weight reduction. The initial design for the usage of the folded heat sink was conducted as follows. The heat sinks are connected in both large surfaces of the cell in order to increase the cooling surface area. The main idea for using the heat sink is increasing the effect of convection heat transfer. The picture of the cell and the setup is revealed in Fig. 1. The setup included an LTO cell embedded with heat sinks, the PEC® battery tester, the TC-08 Pico data logger, a thermal camera, three K-type thermocouples, and a personal computer. All used thermocouples are precisely calibrated with an accuracy of ±0.2 □. The cell surface temperature is recorded by thermocouples in three points for NC. To compare the

different cooling strategies, the cell located inside the room with a controlled constant temperature of 22 °C. The LTO cell was discharged at a high constant current of 8C (184 A) from 100% to 0% of the state of charge.

C. Test Results

1. NC and Cell

NC heat transfer is the first scenario to consider the temperature of the cell. Fig. 2) a shows the location of the thermocouple on the cell surface. Moreover, Fig. 2) b, c displays the thermal image and temperature trend of the cell at the end of the test (446 s) that reaches 56 □. As can be seen, the temperature is non-uniform with a concentration in the center and top of the cell, which is shown by the dashed line. The experimental test results display that cooling by NC is not an effective means for removing heat from the cell surface.

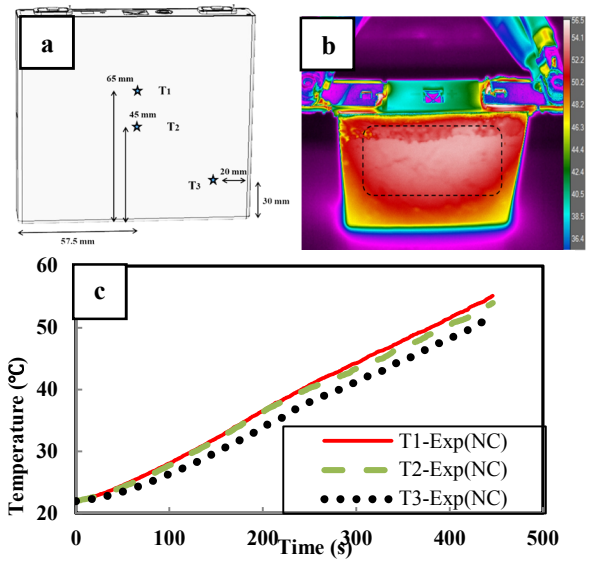

Fig. 2. a) The schematic of the cell with the location of thermocouples, b) the infrared picture, c) temperature trend of thermocouples at the end of the 8C discharging rate test (EXP: Experimental)

2. NC and CHS

In the second scenario, to increase the surface area of the cell, two heat sinks are connected to two sides of the cell (Fig. 3a). In order to maximize the cooling efficiency, the heat sinks are connected to the dashed zone, which presents the hottest zone of the cell. To reduce the contact thermal resistance, gap filler with thermal conductivity of 8 W/m. K is used between the heat sinks and cell. Fig. 3) a and 3) b show the schematic location and temperature trend of thermocouples, respectively.

III. MODEL DEVELOPMENT

A. Modeling Methodology Description

According to the above observations reported in the last section, one can see that the NC strategy is not sufficient to control the temperature of the cell in the 8C discharging rate. Therefore, in order to preserve the cell temperature in a safe zone [4,5] and optimize the whole system, a simulated forced cooling solution is proposed.

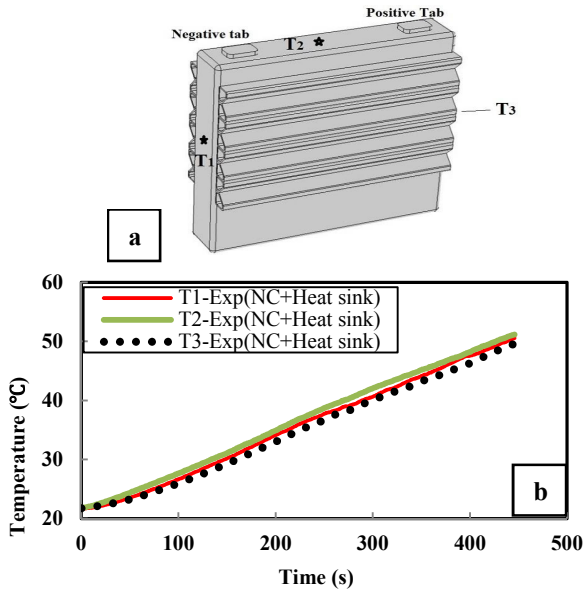

Fig. 3. The schematic of the CHS, a) with the location of thermocouples, b) transient temperature of the CHS at the end of the 8C discharging rate test (446s)

B. Battery Thermal Modeling

The energy balance equation is used to define the transient thermal distribution in the LTO cell. This equation is resulting from the • rst law of thermodynamics. According to this equation, the amount of heat generation inside the cell or transferring from the cell to its ambient is formulated as follows:

$$mC_p \frac{\partial T}{\partial t} + q_{conv} = k\left[\frac{\partial^2 T}{\partial x^2} + \frac{\partial^2 T}{\partial y^2} + \frac{\partial^2 T}{\partial z^2}\right] + q_g \quad (1)$$

where q_g and T de• ne the heat generation and temperature of the cell, respectively. Besides, C_p is the speci• c heat capacity, and k is the 3-Dimensions (3D) thermal conductivity of the cell. The convection heat transfer from the cell to its ambient is calculated as following [24]:

$$q_{conv} = hA(T_{amb} - T_{bat}) \quad (2)$$

where A is the cross-section surface area of the cell and h is the convection heat transfer of coe•cient. Moreover, T_{amb} and T_{bat} are the ambient and battery temperature respectively. The heat generation for the cell and corresponding tabs are calculated as following [27]:

$$q_g = R_{bat}.I^2 \quad (3)$$

$$\dot{q} = R_{tab}.I^2 \quad (4)$$

Where the R_{bat} and R_{tab} are the current, ohmic resistance of the cell and electrical resistance of the tab, respectively.

C. Validation of the Thermal Model

In order to validate the simulation model with experimental data, the temperature of the thermocouples of T2 (Fig. 4) a) and T3 (Fig. 4) b) during 8C discharging mode and initial temperature of 22 • for NC are compared with the simulation results. As it is evident, there is an acceptable agreement between the simulation and experimental results. With the aim of forced convection validation (Fig. 4)c), the accuracy of the numerical model is compared with the experimental air cooling results that were studied by Soltani et al. [28]. The numerical model has been simulated in COMSOL Multiphysics® software. According to the experimental test, the air velocity is set to 5 m/s and

thermocouple placed near the positive tab. As it is evident in Fig. 4) c, there is a perfect agreement between the simulation and experimental data. It is necessary to mention that the variance in temperatures is due to the different ambient temperatures.

D. Simulation Results

1) Natural and Forced Convection

This section presents the simulation results obtained with the cell in natural and forced convection. The main idea is showing the graphical evolution of the cell and CHS in the initial temperature of 22 • under the natural and forced convection conditions. Fig. 5) a display the temperature distribution contour for LTO cell with an NC strategy. It can be seen that in the presence of the NC, the maximum temperature of the cell reaches 55.5 °C with a concentration in the center and top of the cell. Therefore, additional improvement is necessary, as the temperature distribution is non-uniform, and the cell temperature is much higher than the optimal range for Li-ion batteries [4], [5]. According to Fig. 5b usage of the aluminum heat sink has a positive effect on the maximum temperature of the cell. However, the CHS temperature is still out of the safe range. Therefore, the forced convection method can be a solution. The experimental cooling box recommended by Soltani et al. [28] is designed with the same dimensions. The temperature of the CHS with 5 m/s inlet velocity in the forced convection cooling system, (Fig. 5) c) reaches to 31.1 •, which is almost 39.6% temperature reduction compared with the second scenario.

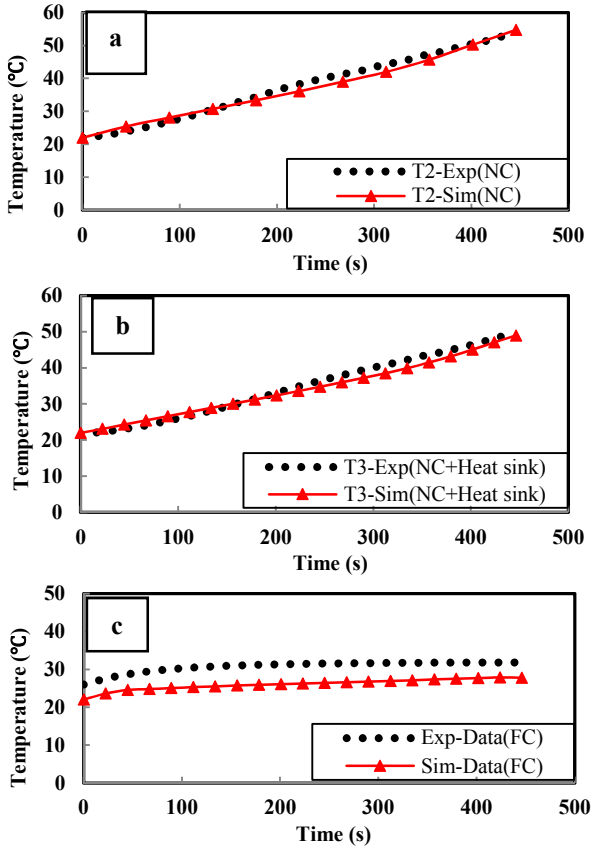

Fig. 4. Thermal model validation of the cell in 8C discharging mode for (a) NC, (b) NC and CHS and (c) forced convection for CHS (EXP: Experimental, Sim: Simulation)

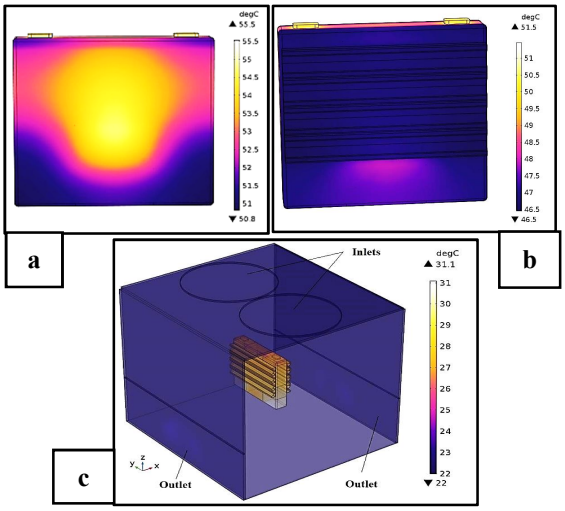

Fig. 5. Temperature contour of the cell in 8C discharging mode for (a) NC, (b) NC with heat sink, and (c) forced convection.

2) The Cooling Effect of Heat Sink Under Forced-Convection

Fig. 6) a and 6) b show the temperature contour of the CHS and velocity of the air around it in the cooling box, respectively.

The heat transfer mechanisms are coupling of the conduction and convection among the cell, heat sink, and air. Despite the low heat transfer coefficient of the air [37], the cooling system is quite successful and keeps the CHS temperature is in a safe zone. However, there is still a temperature difference inside the cell, regardless of the heat sink existence. In fact, the heat migrates from the top of the cell to the down because of forced direct cooling. Therefore, optimization is necessary for the improvement of temperature uniformity inside the cell.

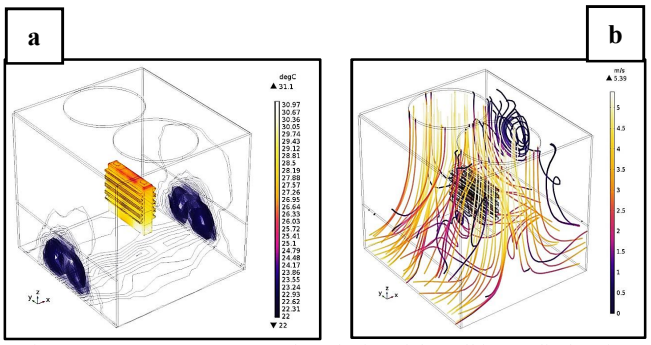

Fig. 6. a) Temperature contour, b) velocity of the cell in 8C discharging mode for forced convection in inlet velocity

3) Optimization of the Outlet Position in Temperature Uniformity

Temperature uniformity inside the cell and the battery pack has an important effect on the performance, efficiency, and lifetime of the cell and the battery pack. As it is mentioned in the last section, the forced convection controlled the CHS temperature in a safe zone. However, the temperature uniformity inside the CHS is not desirable. In this section, the temperature uniformity of CHS has been considered by the different outlet positions. Fig. 7) a, b shows the different cases for outlet positions and 2D cut plane respectively to investigate the temperature uniformity.

According to the results in Fig. 8 the maximum temperature of the CHS in forced convection compared with NC reduced by 39.6%, 40.9%, and 38.4% for cases A, B, and C, respectively. In addition, the results show an improvement of 6%, 28%, and 36% in the temperature uniformity for cases A, B, and C, respectively.

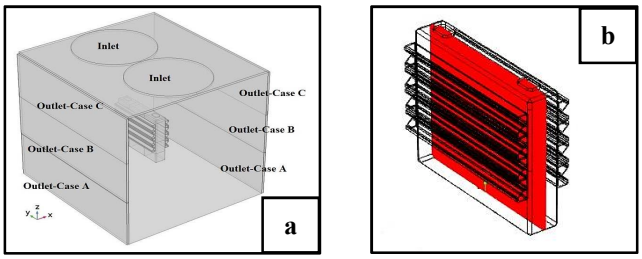

Fig. 7. a) Different outlet positions, b) 2D cut plane for CHS.

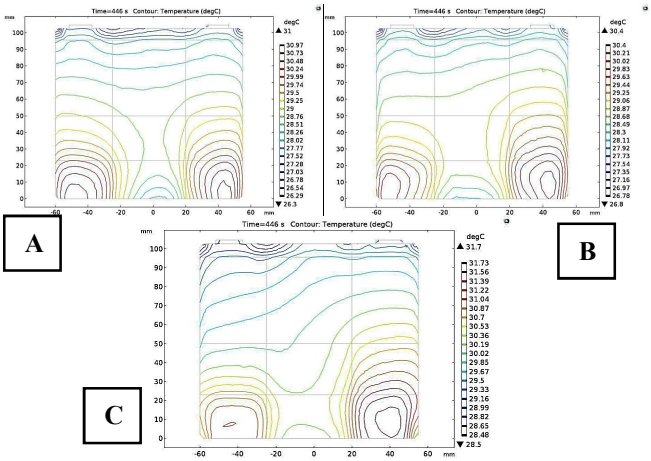

Fig. 8. 2D cut plane temperature contour of CHS for Case A, B, and C for inlet velocity of 5 m/s

4) Optimization of the Different Inlet Velocities and Ambient Temperatures

In the last section, the optimization is done at the geometry level. It was found that the outlet position in case C performed an acceptable result for the maximum temperature and the best results for the temperature uniformity of the CHS. In the current section, the optimization is done with different ambient temperatures and inlet velocities for case C. As it is clear from the results of Table 2, the air velocity of 3 m/s can control the cell in the safe temperature zone. Soltani et al. [28] presented the power consumption of the fan for inlet velocity of 3 and 5 m/s is 6 W and 12 W, respectively. Therefore, there will be a 50% reduction in fan power consumption.

5) Investigation of Module Temperature Consisting of Five Cells

After optimization of outlet and boundary condition, case C and inlet velocity of 3 m/s has been chosen. In order to investigate the effectiveness of the heat sink and air-cooling system on the module temperature, five LTO cells embedded with the heat sink. As can be seen in Fig. 9, the temperature of the module is limited to the range of 33-35.3 •, which shows a safe range [4], [5] at the end of the 8C discharging rate.

TABLE II
OPTIMIZATION OF DIFFERENT VELOCITIES AND AMBIENT TEMPERATURES

Velocity /Temperature	0	10	22	35	45
3 m/s	10.8	20.9	32.9	46	56.1
4 m/s	10.4	20.4	32.5	45.5	55.5
5 m/s	9.6	19.7	31.7	45.1	55.2

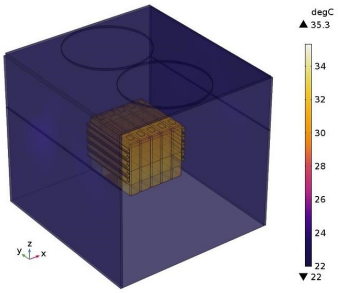

Fig. 9. Temperature contour of equipped the module with the heat sink in 8C discharging mode for forced convection.

IV. CONCLUSION

In this paper, an experimental and numerical study was done to improve the cooling and temperature uniformity of an LTO cell in high current discharging. Several cooling scenarios were developed. In the first and second scenarios, the temperature of the cell and CHS were investigated experimentally in NC. In the third scenario, the effect of forced cooling was considered on CHS temperature. Along with the results, the maximum CHS temperature for the cooling strategy using NC and forced air cooling reaches 51.5 °C and 31.1 °C which can reduce the cell maximum temperature in the first scenario by up to 10% and 44.4% respectively.

Moreover, according to the outlet position optimization, the maximum temperature of the CHS compared with the first scenario decreased by 39.6%, 40.9%, and 38.4% for cases A, B, and C, respectively. Besides, there was an improvement of 6%, 28%, and 36% in the CHS temperature uniformity for cases A, B, and C, respectively. It was concluded that using case C performs the best results for the battery cooling system with a very simple design. As proved, the inlet velocity of 3 m/s is sufficient for cooling, which will be a 50% reduction for fan power consumption. Moreover, the module temperature consisting of five cells limited in a safe temperature range using case C and 3 m/s inlet velocity.

ACKNOWLEDGMENT

This paper was developed under the framework of SELFIE and GHOST projects. These projects have received funding from the European Union's Horizon 2020 research and innovation program under Grant Agreement Nr. 824290 and 770019, respectively. Further, we acknowledge Flanders Make for support to our research team.

REFERENCES

[1] F. Chen *et al.*, "Air and PCM cooling for battery thermal management considering battery cycle life," *Appl. Therm. Eng.*, vol. 173, p. 115154, Jun. 2020.

[2] S. H. Hong, D. S. Jang, S. Park, S. Yun, and Y. Kim, "Thermal performance of direct two-phase refrigerant cooling for lithium-

ion batteries in electric vehicles," *Appl. Therm. Eng.*, vol. 173, p. 115213, Jun. 2020.
[3] S. Lei, Y. Shi, and G. Chen, "A lithium-ion battery-thermal-management design based on phase-change-material thermal storage and spray cooling," *Appl. Therm. Eng.*, vol. 168, p. 114792, Mar. 2020.
[4] M. Pan, X. Zhong, G. Dong, and P. Huang, "Experimental study of the heat dissipation of battery with a manifold micro-channel heat sink," *Appl. Therm. Eng.*, vol. 163, p. 114330, Dec. 2019.
[5] L. H. Saw, Y. Ye, A. A. O. Tay, W. T. Chong, S. H. Kuan, and M. C. Yew, "Computational fluid dynamic and thermal analysis of Lithium-ion battery pack with air cooling," *Appl. Energy*, vol. 177, pp. 783–792, Sep. 2016.
[6] D. Karimi *et al.*, "Thermal performance enhancement of phase change material using aluminum-mesh grid foil for lithium-capacitor modules," *J. Energy Storage*, vol. 30, p. 101508, 2020.
[7] K. Chen, Y. Chen, Z. Li, F. Yuan, and S. Wang, "Design of the cell spacings of battery pack in parallel air-cooled battery thermal management system," *Int. J. Heat Mass Transf.*, vol. 127, pp. 393–401, 2018.
[8] W. Wu, X. Yang, G. Zhang, K. Chen, and S. Wang, "Experimental investigation on the thermal performance of heat pipe-assisted phase change material based battery thermal management system," *Energy Convers. Manag.*, vol. 138, pp. 486–492, Apr. 2017.
[9] K. Chen, Y. Chen, Y. She, M. Song, S. Wang, and L. Chen, "Construction of effective symmetrical air-cooled system for battery thermal management," *Appl. Therm. Eng.*, vol. 166, p. 114679, Feb. 2020.
[10] Y. Fan, Y. Bao, C. Ling, Y. Chu, X. Tan, and S. Yang, "Experimental study on the thermal management performance of air cooling for high energy density cylindrical lithium-ion batteries," *Appl. Therm. Eng.*, vol. 155, pp. 96–109, Jun. 2019.
[11] D. Karimi, H. Behi, J. Jaguemont, M. El Baghdadi, J. Van Mierlo, and O. Hegazy, "Thermal Concept Design of MOSFET Power Modules in Inverter Subsystems for Electric Vehicles," no. January 2020, 2019.
[12] J. Cao, M. Luo, X. Fang, Z. Ling, and Z. Zhang, "Liquid cooling with phase change materials for cylindrical Li-ion batteries: An experimental and numerical study," *Energy*, vol. 191, p. 116565, Jan. 2020.
[13] Y. Lai, W. Wu, K. Chen, S. Wang, and C. Xin, "A compact and lightweight liquid-cooled thermal management solution for cylindrical lithium-ion power battery pack," *Int. J. Heat Mass Transf.*, vol. 144, p. 118581, Dec. 2019.
[14] D. Kong, R. Peng, P. Ping, J. Du, G. Chen, and J. Wen, "A novel battery thermal management system coupling with PCM and optimized controllable liquid cooling for different ambient temperatures," *Energy Convers. Manag.*, vol. 204, p. 112280, Jan. 2020.
[15] M. Behi, S. A. Mirmohammadi, M. Ghanbarpour, H. Behi, and B. Palm, "Evaluation of a novel solar driven sorption cooling/heating system integrated with PCM storage compartment," *Energy*, vol. 164, pp. 449–464, Dec. 2018.
[16] E. B. Haghighi *et al.*, "Cooling performance of nanofluids in a small diameter tube," *Exp. Therm. Fluid Sci.*, vol. 49, pp. 114–122, Sep. 2013.
[17] S. Mirmohammadi and M. Behi, "Investigation on Thermal Conductivity, Viscosity and Stability of Nanofluids," p. 140, 2012.
[18] M. Behi *et al.*, "Experimental and numerical investigation on hydrothermal performance of nanofluids in micro-tubes," *Energy*, vol. 193, p. 116658, Feb. 2020.
[19] M. M. Heyhat, S. Mousavi, and M. Siavashi, "Battery thermal management with thermal energy storage composites of PCM, metal foam, fin and nanoparticle," *J. Energy Storage*, vol. 28, p. 101235, Apr. 2020.
[20] M. Safdari, R. Ahmadi, and S. Sadeghzadeh, "Numerical investigation on PCM encapsulation shape used in the passive-active battery thermal management," *Energy*, vol. 193, p. 116840, Feb. 2020.
[21] H. Behi, "Experimental and numerical study on heat pipe assisted PCM storage system." 2015.
[22] H. Behi, M. Ghanbarpour, and M. Behi, "Investigation of PCM-assisted heat pipe for electronic cooling," *Appl. Therm. Eng.*, vol. 127, pp. 1132–1142, Dec. 2017.
[23] H. Behi *et al.*, "Thermal management analysis using heat pipe in the high current discharging of lithium-ion battery in electric vehicles," *J. Energy Storage*, vol. 32, p. 101893, 2020.
[24] H. Behi *et al.*, "A new concept of thermal management system in Li-ion battery using air cooling and heat pipe for electric vehicles," *Appl. Therm. Eng.*, vol. 174, p. 115280, Apr. 2020.
[25] Y. Ye, Y. Shi, L. H. Saw, and A. A. O. Tay, "Performance assessment and optimization of a heat pipe thermal management system for fast charging lithium ion battery packs," *Int. J. Heat Mass Transf.*, vol. 92, pp. 893–903, Jan. 2016.
[26] Y. Ye, L. H. Saw, Y. Shi, and A. A. O. Tay, "Numerical analyses on optimizing a heat pipe thermal management system for lithium-ion batteries during fast charging," *Appl. Therm. Eng.*, vol. 86, pp. 281–291, Jul. 2015.
[27] J. Jaguemont, L. Boulon, and Y. Dubé, "Characterization and modeling of a hybrid-electric-vehicle lithium-ion battery pack at low temperatures," *IEEE Trans. Veh. Technol.*, vol. 65, no. 1, pp. 1–14, 2016.
[28] M. Soltani *et al.*, "Three dimensional thermal model development and validation for lithium-ion capacitor module including air-cooling system," *Appl. Therm. Eng.*, vol. 153, pp. 264–274, May 2019.